Climate Dynamics (2019) 52:1395–1411
https://doi.org/10.1007/s00382-018-4201-8

Contrasting spatial structures of Atlantic Multidecadal Oscillation between observations and slab ocean model simulations

Cheng Sun[1] · Jianping Li[1,2] · Fred Kucharski[3,4] · Jiaqing Xue[5,7] · Xiang Li[6]

Received: 6 November 2017 / Accepted: 3 April 2018 / Published online: 11 April 2018

Abstract

The spatial structure of Atlantic multidecadal oscillation (AMO) is analyzed and compared between the observations and simulations from slab ocean models (SOMs) and fully coupled models. The observed sea surface temperature (SST) pattern of AMO is characterized by a basin-wide monopole structure, and there is a significantly high degree of spatial coherence of decadal SST variations across the entire North Atlantic basin. The observed SST anomalies share a common decadal-scale signal, corresponding to the basin-wide average (i. e., the AMO). In contrast, the simulated AMO in SOMs (AMO_s) exhibits a tripole-like structure, with the mid-latitude North Atlantic SST showing an inverse relationship with other parts of the basin, and the SOMs fail to reproduce the observed strong spatial coherence of decadal SST variations associated with the AMO. The observed spatial coherence of AMO SST anomalies is identified as a key feature that can be used to distinguish the AMO mechanism. The tripole-like SST pattern of AMO_s in SOMs can be largely explained by the atmosphere-forced thermodynamics mechanism due to the surface heat flux changes associated with the North Atlantic Oscillation (NAO). The thermodynamic forcing of AMO_s by the NAO gives rise to a simultaneous inverse NAO–AMO_s relationship at both interannual and decadal timescales and a seasonal phase locking of the AMO_s variability to the cold season. However, the NAO-forced thermodynamics mechanism cannot explain the observed NAO–AMO relationship and the seasonal phase locking of observed AMO variability to the warm season. At decadal timescales, a strong lagged relationship between NAO and AMO is observed, with the NAO leading by up to two decades, while the simultaneous correlation of NAO with AMO is weak. This lagged relationship and the spatial coherence of AMO can be well understood from the view point of ocean dynamics. A time-integrated NAO index, which reflects the variations in Atlantic meridional overturning circulation (AMOC) and northward ocean heat transport caused by the accumulated effect of NAO forcing, reasonably well captures the observed multidecadal fluctuations in the AMO. Further analysis using the fully coupled model simulations provides direct modeling evidence that the observed spatial coherence of decadal SST variations across North Atlantic basin can be reproduced only by including the AMOC-related ocean dynamics, and the AMOC acts as a common forcing signal that results in a spatially coherent variation of North Atlantic SST.

Electronic supplementary material The online version of this article (https://doi.org/10.1007/s00382-018-4201-8) contains supplementary material, which is available to authorized users.

✉ Cheng Sun
scheng@bnu.edu.cn

✉ Jianping Li
ljp@bnu.edu.cn

[1] College of Global Change and Earth System Science (GCESS), Beijing Normal University, Beijing 100875, China

[2] Laboratory for Regional Oceanography and Numerical Modeling, Qingdao National Laboratory for Marine Science and Technology, Qingdao 266237, China

[3] The Abdus Salam International Centre for Theoretical Physics, Trieste, Italy

[4] Department of Meteorology, Center of Excellence for Climate Change Research, King Abdulaziz University, Jeddah, Saudi Arabia

[5] State Key Laboratory of Numerical Modeling for Atmospheric Sciences and Geophysical Fluid Dynamics, Institute of Atmospheric Physics, Chinese Academy of Sciences, Beijing 100029, China

[6] Key Laboratory of Research on Marine Hazards Forecasting, National Marine Environmental Forecasting Center, State Oceanic Administration, Beijing 100081, China

[7] College of Earth Science, University of Chinese Academy of Sciences, Beijing 100049, China

1 Introduction

The global sea surface temperature (SST) shows a remarkable warming trend over the past century due to the increase of greenhouse gas concentration (Stocker et al. 2013). Overlaying the century-scale warming trend, these is strong variability of global SST at decadal to multidecadal time scales, particularly over the Pacific and Atlantic Oceans. The decadal variability of Atlantic SST is dominated by the Atlantic Multidecadal Oscillation (AMO), which emerges as the first leading empirical orthogonal function (EOF) mode of annual mean SST anomalies over the North Atlantic basin (Delworth et al. 2007). The AMO can also be obtained as one of the leading EOF modes of the global decadally-filtered SST data (McCabe and Palicki 2006; Parker et al. 2007; Chen et al. 2017). It is characterized by a spatially coherent pattern with SST anomalies of uniform sign covering the entire North Atlantic basin. Due to this basin-wide monopole structure, an AMO index can be simply defined as the area-weighted average of Atlantic SST anomalies from the equator northward (Enfield et al. 2001; Sutton and Hodson 2005; Ting et al. 2009). Both reconstructions and observations suggest a quasi-periodic behavior of the AMO, showing oscillations between warm and cold phases with a period of 50–80 years (Schlesinger and Ramankutty 1994; Gray et al. 2004). The climate in the regions surrounding the Atlantic basin is significantly influenced by the AMO (Enfield et al. 2001; Sutton and Hodson 2005; Knight et al. 2006; Ting et al. 2009; Sutton and Dong 2012; O'Reilly et al. 2017), and the AMO also extends its influence across the Eurasian continent to the regions of Siberia and East Asia (Lu et al. 2006; Li and Bates 2007; Sun et al. 2015a, 2017a). The AMO has substantial climate impacts not only over the land surface but also over the ocean, and recent studies have suggested that the AMO plays an important role in the decadal-scale inter-basin interaction between the Atlantic and Indo-Pacific oceans (Zhang and Delworth 2007; Kucharski et al. 2016; Li et al. 2015; Sun et al. 2017b).

Several mechanisms have been proposed to explain the possible source of AMO, including both external forcing (Booth et al. 2012; Ottera et al. 2010; Murphy et al. 2017; Bellomo et al. 2017) and low frequency internal dynamics. One of the most accepted theories is that the AMO is primarily driven by variations in the strength of Atlantic meridional overturning circulation (AMOC) (Delworth and Mann 2000; Knight et al. 2005; Ba et al. 2013; Zhang et al. 2013; Zhang and Wang 2013; Sun et al. 2015b; Vecchi and Delworth 2017). Associated with a strengthening (weakening) of AMOC, the northward oceanic heat transport in the Atlantic is increased (decreased), and this leads to a warm (cold) phase of the AMO. In light of this, the AMO can be largely interpreted as a result from ocean dynamics, and thus an internal mode of climate variability. The observational record of deep ocean circulation is too short to analyze the direct link between the AMOC and AMO at multidecadal time scales. Nevertheless, there is increasing observational evidence supporting the AMOC-AMO link by use of proxies of the AMOC strength, including the leading mode of extratropical subsurface temperature at 400 m (Zhang 2008), seawater density (Wang et al. 2009), sea level gradient (McCarthy et al. 2015), upper ocean heat content (Robson et al. 2012; Chen and Tung 2014; McCarthy et al. 2015) and subpolar sea surface salinity (Zhang 2017). Meanwhile, several dynamical mechanisms have been proposed to explain the quasi-periodic multidecadal variability of the AMOC and AMO, such as a self-sustained or damped oscillation arising from dynamical ocean processes excited by stochastic atmospheric forcing (Dijkstra et al. 2006) and a delayed oscillator resulting from the decadal-scale atmosphere–ocean interactions in the North Atlantic (Sun et al. 2015b).

The AMOC-related ocean dynamics mechanism for the AMO has been recently challenged by the atmosphere-forced thermodynamics mechanism proposed by Clement et al. (2015). They analyzed the Atlantic SST multidecadal variability from Coupled Model Intercomparison Project Phase 3 (CMIP3) preindustrial control simulations run with a slab ocean model (SOM; 50-m-deep mixed layer ocean model), in which only the thermally coupling between atmosphere and ocean is considered while the role of ocean circulation change and associated ocean heat transport is absent. They also compared the results with both fully coupled model simulations and SST observations and claimed that the SOMs are capable of reproducing the main features of AMO without a role for ocean circulation. Their findings suggest that the AMO is mainly a direct response of North Atlantic SST to the stochastic atmospheric forcing, and thus the key process involved can be largely interpreted as a red-noise process. In contrast to the view of atmospheric thermodynamic forcing, Zhang et al. (2016) argued that fully coupled models reproduce the observed inverse relationship between net downward surface heat flux and SST anomalies over subpolar North Atlantic at decadal time scales (Gulev et al. 2013). This indicates that at long time scales the surface temperature and heat fluxes are driven by the ocean, rather than the converse. This inverse relationship has also been identified as a key feature associated with the AMO by other studies (O'Reilly et al. 2016; Drews and Greatbatch 2016; Zhang 2017), which further used this feature to distinguish the relative roles of oceanic versus atmospheric forcing and demonstrated the central role of the ocean dynamics mechanism. More recent studies (Clement et al. 2016; Cane et al. 2017) have suggested that the

negative correlation between net surface heat flux and SST anomalies at low frequencies is a consequence of the surface heat balance being in near equilibrium at long time scales, and that the correlation does not distinguish between the atmospheric and oceanic forcing as the source of the AMO. However, Zhang (2017) shows that the negative correlation and regression between net surface heat flux and subpolar North Atlantic SST anomalies at low frequencies are key indicators of the oceanic forcing in SST anomalies, and that the red noise model with no oceanic damping (Clement et al. 2015; Cane 2017) leads to the unrealistic interpretation of the negative correlation.

Identification of a key feature associated with the AMO that distinguishes the two mechanisms is crucial for understanding the physical nature of AMO. Since the SOMs only provide ocean variables at the air–sea interface, a detailed comparison of the spatio-temporal features of AMO SST anomaly between observations and SOMs could be a direct and effective way. Analyses of reconstructions and observational records have suggested a strong spectral peak of 50–80 years in the AMO index (Gray et al. 2004; Schlesinger and Ramankutty 1994). Although the SOM can indeed simulate multidecadal variability over the North Atlantic (Clement et al. 2015, 2016) as part of a red noise process, the quasi-periodic temporal feature associated with the AMO cannot be simulated and explained by the red-noise process as revealed in the SOMs. For the North Atlantic SST anomalies simulated in SOMs, there is no enhanced power at the multidecadal time scale above the red noise background as that observed (Zhang 2017). Both temporal and spatial features need to be considered to fully characterize the AMO phenomenon. In this context, it may be insufficient to consider the temporal feature only, and further investigations are needed focusing on the spatial feature associated with the AMO. In the literature, the AMO is described as a SST homogenous pattern over the North Atlantic (Enfield et al. 2001), but the degree of spatial coherence of the multidecadal SST anomalies across the entire basin has not been quantified and examined across different observational SST data sets. Meanwhile, it is still unknown whether the SOMs reproduce the observed spatial coherence associated with the AMO. Therefore, there is a clear need to compare the spatial characteristics of AMO in the observations with the SOMs, and it may provide an additional key feature to distinguish the AMO mechanism and further to understand the physical nature of AMO.

The aim of this study is to identify the spatial coherence associated with the AMO in the observations and compare with the SOMs. Our findings suggest that the observed spatial feature of AMO is inconsistent with the SOM results and thus could be used to distinguish the AMO mechanism. The remainder of this paper is organized as follows. The datasets and methodology are described in Sect. 2. The contrasting spatial structures of AMO between observations and SOM simulations are presented in Sect. 3, and different driving mechanisms responsible for the contrasting spatial features are thoroughly analyzed. Finally, the main conclusions and a discussion are given in Sect. 4.

2 Data and methodology

Data from the CMIP3 models coupled to a slab mixed layer ocean model (hereafter referred to as the SOMs) with a prescribed ocean heat transport are employed, and only the six models that provided at least 60 years of output are analyzed. This restriction secures a long enough sample size for the analysis of multidecadal variability and to provide a relevant comparison with the observations in terms of the statistical significance of correlations. The six SOMs (simulation length in years) analyzed are as follows: MPIM-ECHAM5 (100), GFDL-CM2.1 (100), NASA-GISS-ER (120), INM-CM3 (60), MRI-CGCM2-3-2 (150) and UKMO-HADGEM1 (70). For each model, the pre-industrial control integrations conducted with the fully coupled version of the model are also analyzed to identify the role of ocean dynamics. The simulation lengths (in years) of the fully coupled models are as follows: MPIM-ECHAM5 (506), GFDL-CM2.1 (500), NASA-GISS-ER (500), INM-CM3 (330), MRI-CGCM2-3-2 (350) and UKMO-HADGEM1 (240). Description of these models and experimental designs are available from the CMIP website (http://www-pcmdi.llnl.gov/ipcc/about_ipcc.php). Monthly mean fields from the model output are interpolated to the T42 grid, and the annual cycle are removed before calculating the January to December averaged annual mean anomalies.

Three data sets of global observational SST employed in this study are the Kaplan SST (Kaplan et al. 1998), the Hadley Centre SST (HadSST3, Kennedy et al. 2011) and the extended reconstruction SST version 3 (ERSST v3b, Smith et al. 2008), and two data sets of observational land surface air temperature (LSAT) from Climate Research Union version 3.23 (CRU, Harris et al. 2014) and University of Delaware version 3.01 (UDEL, Willmott and Matsuura 2001) are also used. Because uncertainties in surface observations prior to 1900 are relatively large and the data before 1900 are deemed less reliable, we confine our analysis to the post-1900 period for the datasets (1900–2015). We remove the long-term linear trend in the variables using the least squares method, and our intent is to remove the centennial scale trends to better isolate and highlight the signal of decadal to multidecadal variability. In the literature, there are various methods for isolating observed internal SST variability over the North Atlantic, such as removing the global mean SST (Trenberth and Shea 2006) or subtracting the global mean SST outside the North Atlantic (Sutton and Dong 2012). In

this study, the results based on the three methods above are qualitatively similar, and thus we show the results based on the removal of linear trend. The AMO index in both observations and model simulations is defined as the area-weighted average of SST anomalies over the North Atlantic region (0°–60°N, 80°W–0°).

Two observed annual NAO indices are used in this study. One is defined as the difference in the normalized sea level pressure (SLP) zonally averaged over the North Atlantic sector from 80°W to 30°E between 35°N and 65°N with the base period 1961−1990 (Li and Wang 2003), and it is referred to as NAO_{dif}. The other one is the principal component (PC)-based NAO (Hurrell 1995), which is provided by the Climate Analysis Section of NCAR and referred to as NAO_{pc}. The two NAO indices are both derived from the NCAR SLP data set (Trenberth and Paolino 1980) for the period 1900–2015. Although there are very slight differences between the two indices, the variations in them are largely consistent and the correlation between them is high. As the results based on the two NAO indices are similar, here we mainly show the results based on the NAO_{pc} unless specified otherwise.

Since this study focuses on the time scale of decades, the data are decadally smoothed by using an 11-year running mean filter in most of the analyses. The decadally filtered time series are autocorrelated and thus the effective independent sample size is reduced. The statistical significance of the linear regression coefficient and correlation between two auto-correlated time series is accessed via a two-tailed Student's t test using the effective number of degrees of freedom (Li et al. 2013). The effective number of degrees of freedom N^{eff} is given by the following approximation:

$$\frac{1}{N^{\text{eff}}} \approx \frac{1}{N} + \frac{2}{N}\sum_{j=1}^{N}\frac{N-j}{N}\rho_{XX}(j)\rho_{YY}(j), \tag{1}$$

where N is the sample size and $\rho_{XX}(j)$ and $\rho_{YY}(j)$ are the autocorrelations of two sampled time series X and Y at time lag j.

3 Results

Figure 1 shows the correlation maps between the decadal AMO index and North Atlantic SST anomalies in the observation and simulations from SOMs and fully coupled models. The correlation maps based on the three SST observational datasets display very consistent results (Fig. 1a; Fig. S1 of the Supplementary Material), and all are characterized by a basin-wide monopole structure with highly positive correlations (above 0.7) over the entire North Atlantic

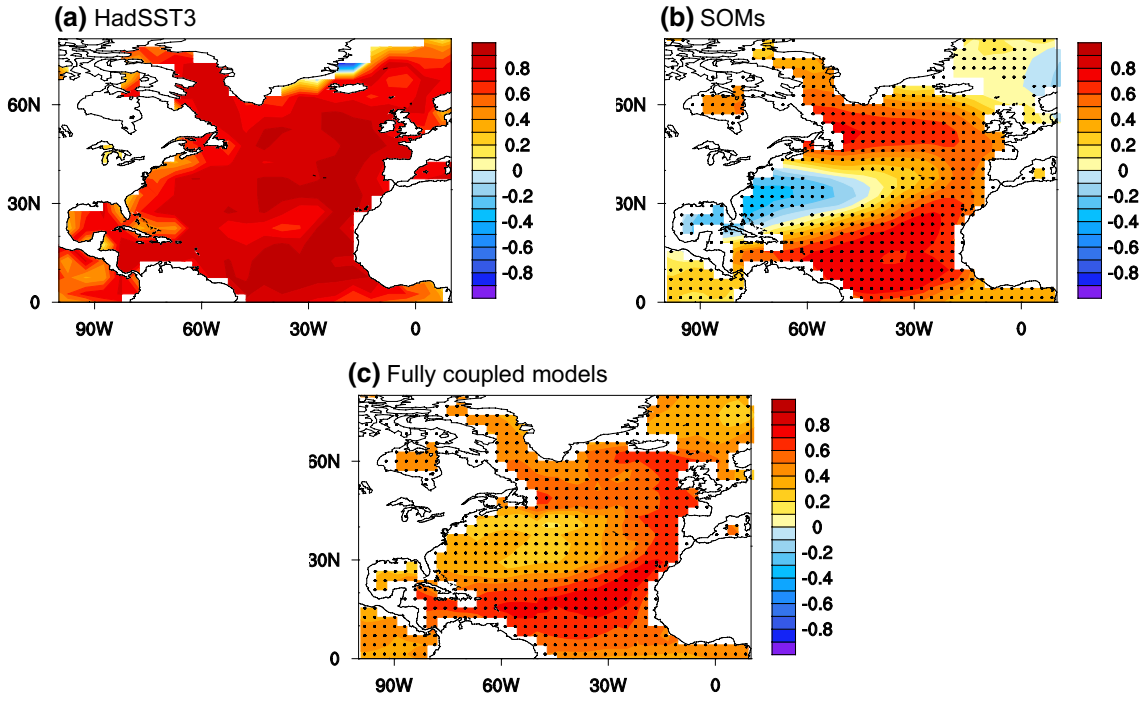

Fig. 1 **a** Correlation map between decadally filtered AMO index and North Atlantic SST anomalies for the period 1900–2015 based on the HadSST3 data set. **b** Multi-model ensemble mean correlation of decadally filtered AMO_s with North Atlantic SST anomalies based on the six slab ocean model simulations (see Sect. 2). Dots in **b** denote the area where at least four of the six models agree on the sign of the correlations. **c** As in **b**, but for the results based on the six fully coupled model simulations

basin. This indicates that the SST anomalies in each part of the basin show similar variations with the AMO at decadal timescales. Previous studies have suggested that the SST over tropical North Atlantic (TNA) exhibits strong interannual variability, which is linked to the El Niño-Southern Oscillation phenomenon (Deser et al. 2010; García-Serrano et al. 2017). After a decadal low-pass filtering is applied, the interannual component of TNA SST is filtered out and the decadal component presents similar variations with the AMO and other parts of the North Atlantic. It is also noted that the spatial structure of the correlation map is slightly different from the regression map of decadal SST anomalies onto the AMO index, which exhibits a horseshoe-like structure with weak positive SST anomalies over the Gulf Stream extension (GSE) region but much stronger positive anomalies over other parts of the basin (Clement et al. 2015). Thus, the correlation map here confirms a strong in-phase relationship between the GSE decadal SST anomalies and the AMO.

The correlation map of Atlantic decadal SST anomalies with the AMO in the SOMs is substantially different from that in the observations. The multi-model ensemble (MME) mean of the SOMs is analyzed here. As seen in Fig. 1b, there are obvious inverse correlations between the GSE decadal SST anomalies and the AMO in the SOMs, while over other parts of the basin the positive correlations remains, corresponding to a tripole-like structure. This result is qualitatively consistent with the regression map of simulated SST anomalies onto the AMO index in the SOMs as shown in Clement et al. (2015), in which the GSE region is dominated by clearly negative SST anomalies with an amplitude of about 0.05 K. Moreover, the inverse relationship of the GSE decadal SST anomalies with the AMO becomes even more clear in the correlation map. However, this noticeable difference in the SST anomaly pattern of AMO between observations and SOMs has not been discussed yet. Due to this difference, the AMO in the SOMs is referred to as AMO_s to distinguish with the observed AMO.

To further illustrate the spatial synchronization of Atlantic decadal SST anomalies as a unique feature of the AMO, we analyzed the cross correlations between the regionally (80°W–0°) zonal-average SST anomalies at various latitudes over the North Atlantic basin. The results from the three observational datasets are consistent with each other (Fig. 2; Fig. S1 of the Supplementary Material). The most remarkable feature is the highly positive correlations of SST anomalies between the TNA, mid-latitude and subpolar North Atlantic basin. This indicates that the SST anomalies at various latitudes of North Atlantic strongly synchronize with each other at decadal timescales. The SST anomalies across the entire North Atlantic basin share a common decadal-scale signal, which could be well captured by the spatial average of SST anomalies, i. e. the AMO. However, the cross correlation of SST anomalies in the SOMs shows a contrasting feature (Fig. 2b). Although the decadal SST anomalies over the TNA and subpolar basin are positively correlated, the mid-latitude (25°–45°N) North Atlantic SST shows an inverse relationship with other parts of the basin at decadal timescales. The decadal SST variability is characterized by a tripole-like pattern in the SOMs, rather than the monopole structure in the observations. Thus, only the SST anomalies in TNA and subpolar basin share a common decadal-scale signal (the basin-average SST anomalies, i.e., the AMO_s), suggesting a lack of spatial coherence in the SOMs. This is consistent with the spatial characteristics of the AMO_s as shown in Fig. 1b. Therefore, there is a high degree of spatial coherence of decadal SST variations over the North Atlantic in the observations, but this observed key feature is clearly absent in the SOMs.

Figure 3 further shows the correlations of the GSE (25°–45°N, 80°–40°W) regionally averaged SST anomalies with the entire basin at decadal timescales. As indicated by the observational results (Fig. 3; Fig. S1 of the Supplementary Material), the SST anomalies over the GSE region exhibit a strong in-phase relationship with other parts of the basin, further supporting that the SST anomalies across the basin share a common decadal-scale signal. However, this is not the case in the SOMs (Fig. 3b), in which negative SST correlations are seen outside the GSE region, in sharp contrast with the observational results. Therefore, the results shown in Fig. 3 are consistent with Figs. 1 and 2, and all indicates that the observed AMO shows a high degree of spatial coherence, characterized by a monopole structure across the basin, while the AMO_s is marked by a tripole-like structure with the lack of spatial coherence.

Different from the SOMs, the fully coupled models qualitatively reproduce the observed spatial coherence of AMO SST anomalies. The MME means of North Atlantic SST correlations with the AMO (Fig. 1c) and cross correlations for the zonal-average SST (Fig. 2c) in the fully coupled models suggest a monopole structure of simulated decadal SST anomalies associated with the AMO. Meanwhile, the MME mean of SST correlations with the GSE regionally averaged SST (Fig. 3c) also shows a positive pattern of correlation between the GSE region and other parts of the basin. Therefore, the spatial feature of simulated AMO SST anomalies in most of the fully coupled models is qualitatively similar to that observed, while significantly contrasting with the tripole-like structure of the AMO_s in the SOMs.

The mechanism that is responsible for the tripole-like structure of the AMO_s is further investigated using the SOM simulations. Figure 4a, b show the decadal atmospheric circulation anomalies (SLP and zonal wind) associated with the AMO_s over the North Atlantic. The SLP field is characterized by a meridional dipole pattern with an anomalous low south of 60°N and an anomalous high north of

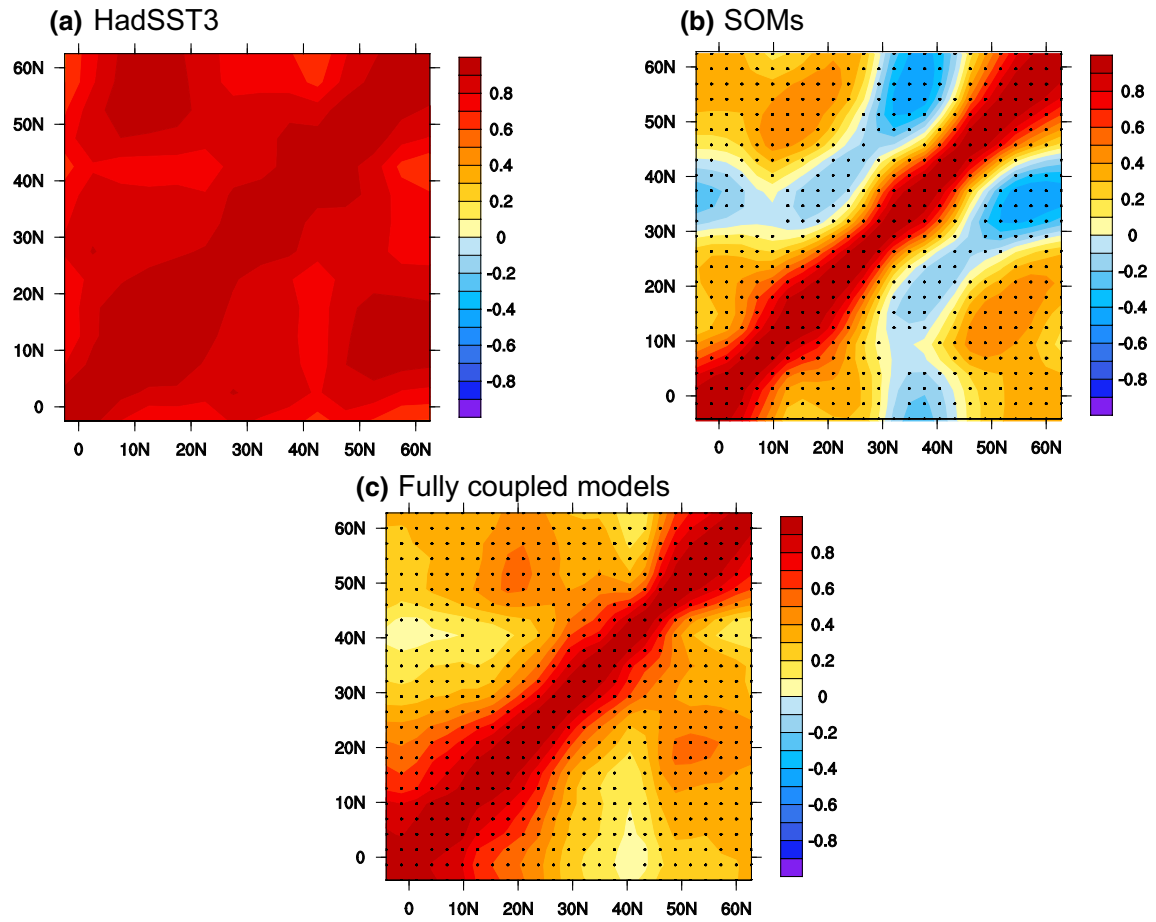

Fig. 2 **a** Cross-correlation coefficients between decadally filtered zonal-average SST anomalies over the North Atlantic (80°W–0°) during 1900–2015 based on the HadSST3 data set. **b** Multi-model ensemble mean cross-correlation coefficients between decadally filtered zonal-average SST anomalies over the North Atlantic (80°W–0°) based on the six slab ocean model simulations. Dots in **b** denote the area where at least four of the six models produce the same sign correlations. **c** As in **b**, but for the results based on the six fully coupled model simulations

60°N, which is similar to the pattern of SLP anomalies during the NAO negative phase. The low and high anomalies correspond to anomalous cyclonic and anti-cyclonic flows, respectively. Thus, the zonal wind field shows westerly anomalies over TNA and mid-latitude North Atlantic (south of 45°N) and easterly anomalies over high-latitude basin centered around 60°N. The atmospheric circulation associated with the AMO_s closely resembles a negative NAO-like pattern, and thus the relationship between AMO_s and NAO in the SOMs is further analyzed. The NAO in each SOM is defined as the leading empirical orthogonal function (EOF) of monthly North Atlantic regional (90°W–40°E) SLP anomalies poleward of 20°N. Figure 4c shows the lead–lag correlations between the decadal AMO_s and NAO in each of the six SOMs and the MME mean of the correlations. All the six models exhibit a negative correlation between decadal AMO_s and NAO at zero lag, and four models show a maximum negative correlation peaking at (or near) zero lag. The MME mean is marked by a clear correlation peak (the maximum correlation reaching −0.52) appearing at zero lag. Figure 4d further shows the lead–lag correlations between the unfiltered AMO_s and NAO. The correlations in the individual models and the MME mean of the correlations are both characterized by a peak with a maximum negative correlation occurring at zero lag. Therefore, there is a simultaneous inverse relationship between the AMO_s and NAO, and this relationship is independent of the low-pass filtering.

Extensive observational studies have suggested that the NAO-related heat flux can force a tripole-like pattern of SST anomalies over the North Atlantic (Cayan 1992; Marshall et al. 2001; Deser et al. 2010). This thermodynamic effect of the stochastic NAO forcing on the SST is reasonably well simulated by the SOMs, in which the SST variation is primarily driven by the net heat flux into the ocean. As shown in Fig. 5, surface wind changes associated with the NAO (Fig. 5a) can lead to a tripole-like pattern of surface turbulent heat flux anomalies (Fig. 5b), which contributes most to the net surface heat flux anomalies (Fig. 5c). As

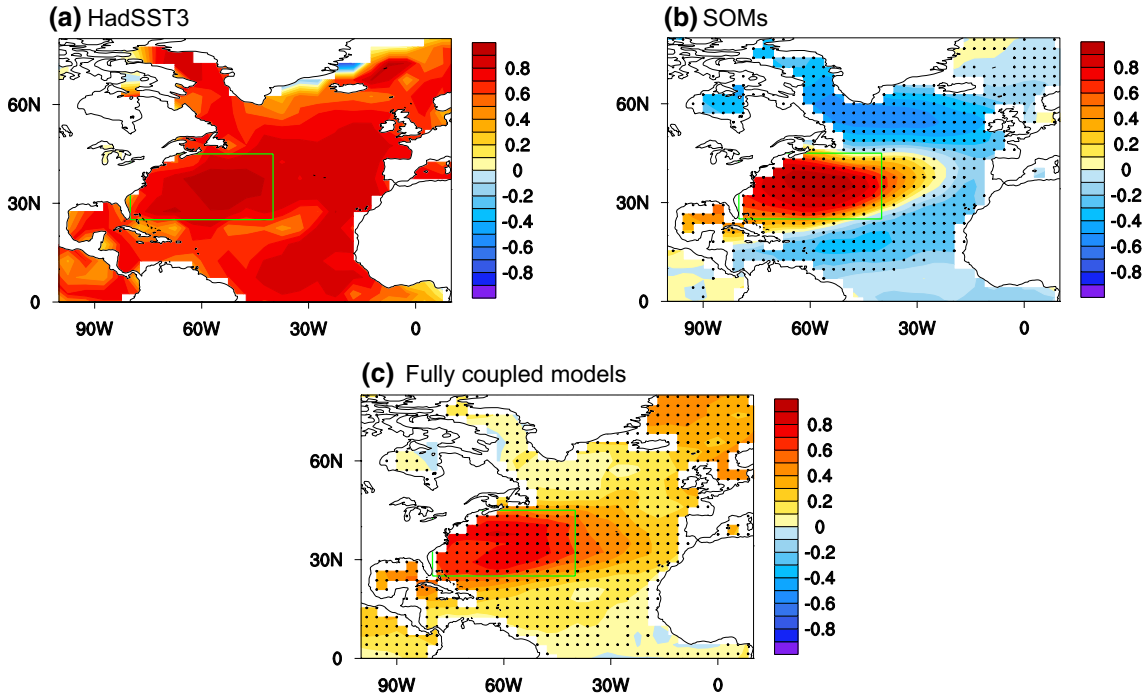

Fig. 3 **a** Correlation map between decadally filtered SST anomaly over the GSE region (25°–45°N, 80°–40°W) and North Atlantic SST anomalies for the period 1900–2015 based on the HadSST3 data set. **b** Multi-model ensemble mean correlation of SST anomaly over the GSE region with North Atlantic SST anomalies based on the six slab ocean model simulations. The green box in **a, b** indicates the GSE region, and dots in **b** denote the area where at least four of the six models agree on the sign of the correlations. **c** As in **b**, but for the results based on the six fully coupled model simulations

a result, the simulated SST anomalies associated with the NAO show a consistent tripole-like structure (Fig. 5d) and look similar to the AMO_s shown in Fig. 1b, further demonstrating the inverse relationship between the AMO_s and NAO in the SOMs.

We further construct a simple stochastic climate model to interpret the relationship between the AMO_s and NAO in the SOM. As indicated in the above thermodynamic analysis, the surface heat flux forcing associated with the negative (positive) NAO phase could induce a warm (cold) phase of AMO_s. Therefore, the model equation is as follows:

$$\frac{d\mathrm{AMO_s}}{dt} = -\mathrm{NAO} - \frac{\mathrm{AMO_s}}{\beta}, \tag{2}$$

where $-\frac{\mathrm{AMO_s}}{\beta}$ is a damping term to represent the persistence and/or reemergence of North Atlantic SST anomalies, and β denotes the timescale of the damping, which is related to the mixed layer depth (Deser et al. 2003, 2010; O'Reilly et al. 2016). The simulation results from this model could represent North Atlantic mixed-layer temperature response to random variations in the NAO-related surface heat flux forcing. Here, we consider two cases with damping timescale β equal to 6 months and 5 years, approximately corresponding to a shallow (50 m) and a deep (500 m) mixed layer, respectively. Over the whole North Atlantic basin, the mixed-layer depth varies considerably, and the mixed layers are usually deeper in the subpolar North Atlantic than in the tropical region. The two cases (a shallow and a deep mixed layer) considered here span the typical range of observed mixed-layer depths across the North Atlantic for which 50 m is typical of the tropical North Atlantic and 500 m representative of the condition in subpolar North Atlantic (Deser et al. 2003, 2010). Thus, the simulations of the simple model aim to illustrate examples of how the AMO_s SST anomalies over North Atlantic responds to the NAO thermodynamic forcing. Figure 6a, b show the input random NAO forcing time series (a Gaussian white noise process with zero mean and unit variance) and the simulated AMO_s responses for the two cases over a 1000-year simulation period. The low-pass filtered NAO, which can be taken as the decadal residual of the interannual fluctuations, appears to be approximately in an anti-phase relationship with the simulated AMO_s. The lead–lag correlations of the NAO with the AMO_s (Fig. 6c, d) show high and significant simultaneous negative correlations for both unfiltered and decadally smoothed time series, indicating that the relationship of NAO with the AMO_s is largely inverse. Particularly, the negative correlation between the NAO and AMO_s peaks at zero lag for the case β equal to 0.5 year, while for the case β

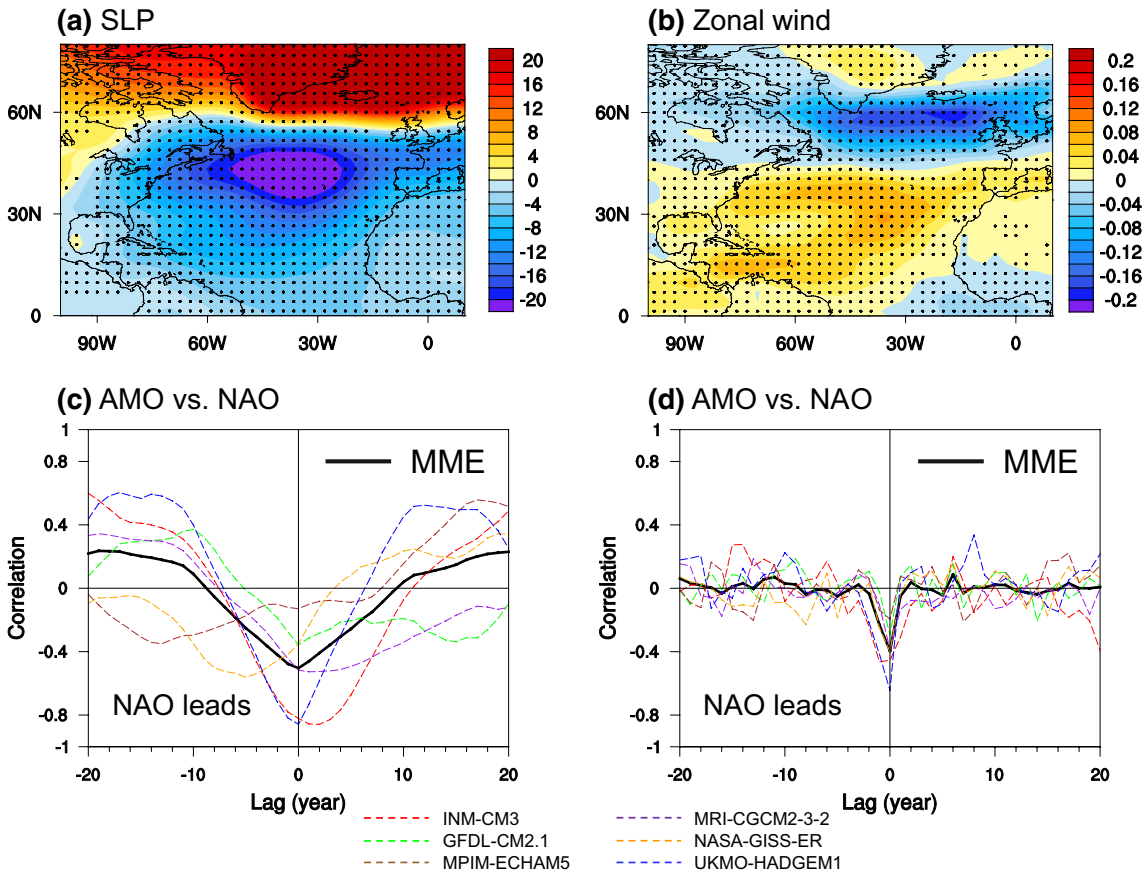

Fig. 4 Multi-model ensemble mean regressions of North Atlantic **a** SLP (Pa) and **b** zonal wind (m s^{-1}) anomalies onto the normalized AMO_s index at decadal timescales based on the six slab ocean model simulations. Dots in **a** and **b** denote the area where at least four of the six models agree on the sign of the regressions. **c** Lead–lag correlations between the decadally filtered AMO_s and NAO indices in the six slab ocean model simulations (dashed lines in colors) and the multi-model ensemble mean (black solid line). Negative (positive) lags indicate NAO leading (lagging) AMO_s. **d** As in **c**, but for the unfiltered indices

equal to 5 years, the negative correlation is not only simultaneous but is also significant and larger when the NAO leads by up to several years due to increased persistence of SST anomalies. Therefore, the NAO–AMO_s relationship estimated from the theoretical stochastic model is consistent with that revealed in the SOMs. This further supports that the AMO_s is largely a thermodynamic response of the ocean to the NAO-related surface heat flux forcing and thus shows a tripole-like spatial pattern.

The thermodynamic forcing of AMO_s by NAO is also reflected in the seasonality in the amplitudes of AMO_s and NAO. As shown in Fig. 7b, the variability of NAO in the observations is strong during cold season (a maximum amplitude in February) but weak during warm season (a minimum in July). The SOMs qualitatively reproduce the seasonality in the NAO amplitude (Fig. 7a), though there is a 1–2 month lag compared to observations and the seasonal variation of the amplitude is weaker than the observations. There is a clear phase locking of AMO_s SST anomalies to the seasonal cycle of the NAO amplitude, with large amplitudes of SST anomalies in cold season and relatively small amplitudes in warm season (Fig. 7c). Thus, the stronger (weaker) the NAO forcing, the stronger (weak) the thermodynamic response in the AMO_s, consistent with the NAO-forced thermodynamic mechanism. However, this is not the case for the observed AMO. In the observations, there is a clear phase opposition between the seasonal cycle of the amplitudes of NAO and AMO (Fig. 7d); that is, the observed AMO shows maximum variability during warm season (when the NAO variability is weak) and minimum variability during cold season (when the NAO variability is strong). Therefore, the NAO-forced thermodynamic mechanism cannot explain the seasonality in the observed AMO amplitude.

The fully-coupled model simulated seasonality in the amplitudes of AMO and NAO is qualitatively consistent with that observed but different from the SOMs. As shown in Fig. 7e, f, the MME mean seasonal cycle of simulated AMO in the fully coupled models shows maximum variability during warm season and relatively weak variability during cold season, almost opposite to the simulated NAO.

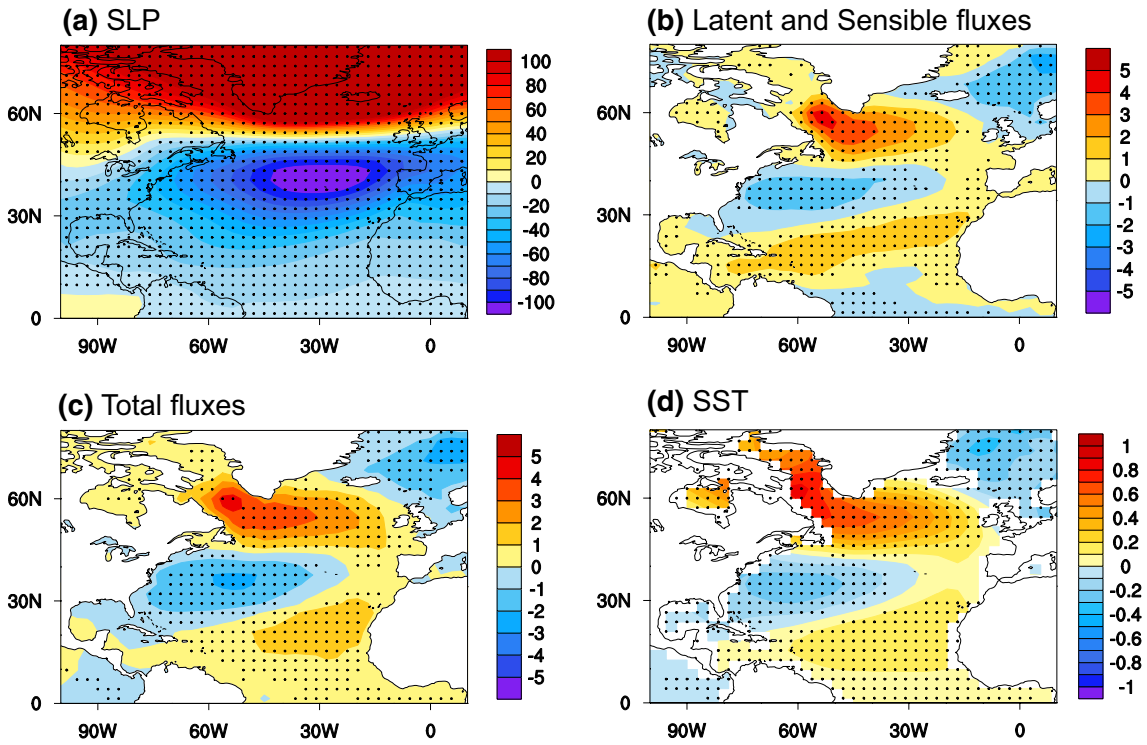

Fig. 5 Multi-model ensemble mean regressions of North Atlantic **a** SLP (Pa), **b** surface turbulent fluxes (latent and sensible heat fluxes, W m^{-2}), **c** total fluxes (the sum of the radiative and turbulent fluxes at the surface, W m^{-2}) and **d** SST (K) onto the normalized annual mean NAO index based on the six slab ocean model simulations. The sign of the NAO index is reversed here, and all surface fluxes are defined positive downward. Dots in **a**–**d** denote the area where at least four of the six models agree on the sign of the regressions

This also indicates that the simulated seasonality of AMO amplitude in most of the fully coupled models cannot be interpreted by the NAO-forced thermodynamic mechanism that operates in the SOMs. In addition, the fully-coupled model simulated NAO–AMO relationship also significantly differs from the NAO–AMO_s relationship in the SOMs. Figure 8a shows the MME mean of decadal SLP anomalies associated with the AMO in the fully coupled models, which exhibits a basin-wide homogeneous pattern dominated by negative SLP anomalies, largely due to the strong surface heating induced by SST warming. The anomalous low associated with AMO was also found in previous observational and modeling studies (Knight et al. 2006; Kucharski et al. 2016; Sun et al. 2017b), and it is obviously contrasting with the NAO-like dipole pattern associated with AMO_s in the SOMs. The simulated lead–lag correlation between decadal NAO and AMO is also examined for comparison (Fig. 8b). In most of the fully coupled models, the lead–lag correlation shows positive correlations at negative lags peaking around lag − 10 years and suggests a decadal lead of NAO relative to the AMO, which is significantly different from the simultaneous inverse relationship found in the SOMs.

The observed NAO–AMO relationship is further analyzed. Figure S2 of the Supplementary Material shows the observed time series of annual NAO_{dif} and NAO_{pc} and the decadally filtered components, showing a high correlation between the two versions of NAO index (r = 0.97). The observed lead–lag correlation between the AMO and NAO (Fig. 9a; Figure S2 of the Supplementary Material) indicates that the NAO leads the AMO by up to two decades (slightly longer than the lead time found in the fully coupled models). It is also noted that there is a simultaneous negative correlation between NAO and AMO for the unfiltered indices, indicating a potential influence of NAO-related heat flux on the AMO at the interannual timescales (Gulev et al. 2013; O'Reilly et al. 2016). However, the correlation between the decadal NAO and AMO at zero lag is very low (around − 0.2) and insignificant. This suggests that the observed decadal variability of AMO cannot be explained by the NAO-forced thermodynamic mechanism.

The observed decadal-scale lag correlation between the NAO and AMO can be interpreted by the ocean dynamics mechanism. To highlight the NAO-related ocean dynamics, a time-integrated NAO index (iNAO) in the observation is calculated based on the following equation:

$$\mathrm{iNAO}(t) = \int_{t_0}^{t} \mathrm{NAO}(t)dt,$$

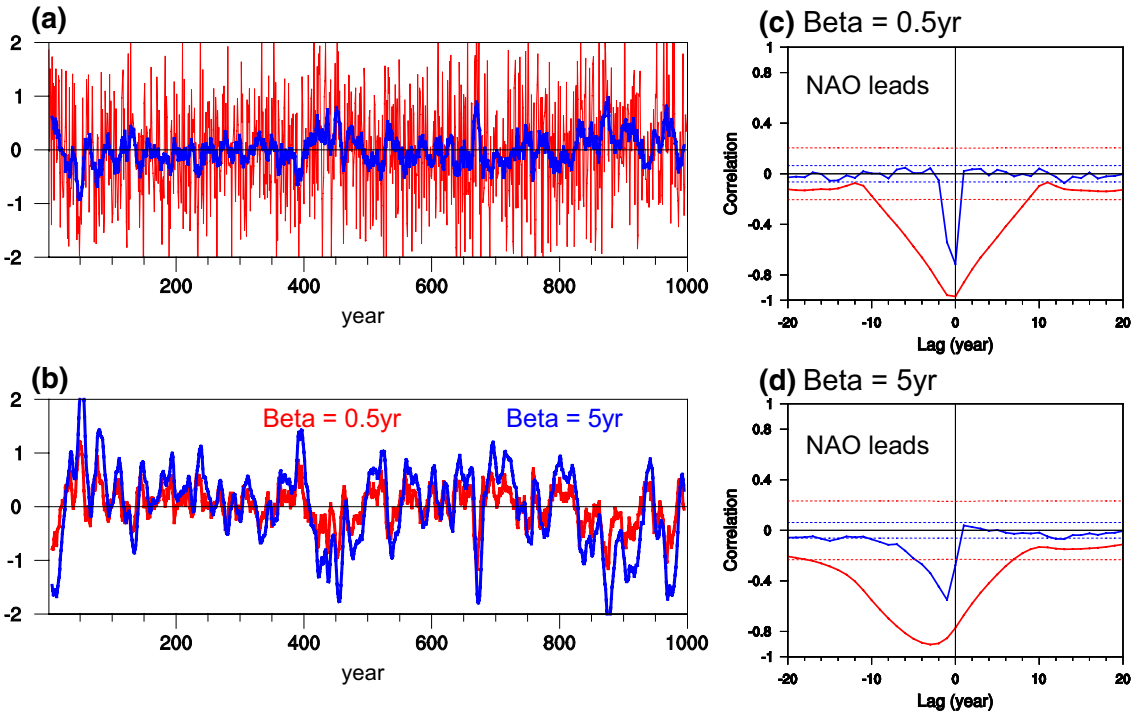

Fig. 6 Numerical simulations of the simple stochastic model (Eq. 2). **a** The time series of the input NAO forcing represented by a 1000 year long white noise. The red (blue) line is the annual mean (decadally filtered) time series. **b** Decadal time series of the output AMO_s responses for the cases $\beta = 0.5$ year (red) and $\beta = 5$ years (blue). **c** Lead–lag correlations between the NAO forcing and simulated AMO_s response for the case $\beta = 0.5$ year based on decadally filtered (red) and unfiltered (blue) time series. Negative (positive) lags indicating the NAO leading (lagging) AMO_s. Red (blue) dashed lines denote the 95% confidence levels for filtered (unfiltered) time series using the effective numbers of degrees of freedom. **d** As in **c**, but for the case $\beta = 5$ years

where t_0 corresponds to the starting year 1900 and t represents the years after 1900. Previous modeling and observational studies have suggested that the iNAO can be considered as a good indicator of the AMOC (Li et al. 2013; Sun et al. 2015b; Mecking et al. 2013, 2015; McCarthy et al. 2015). Li et al. (2013) and Sun et al. (2015b) found that the AMO and related surface air temperature variations lag the NAO by one to two decades due to large ocean inertia associated with the AMOC-related dynamical process, and the temperature multidecadal variability observed in Atlantic and entire Northern Hemisphere can be well captured by integrating the NAO signal (Li et al. 2013). Mecking et al. (2013, 2015) suggested that a simple statistical model based on the iNAO (in a form of cumulative sum of NAO) can be applied to reconstruct the AMOC at 30°N, and this NAO-reconstructed AMOC is highly correlated with the simulated AMOC in a global ocean general circulation model, in which the ocean is driven by the NAO-related atmospheric forcing. McCarthy et al. (2015) showed that the iNAO explains the multidecadal changes in the Atlantic meridional ocean heat transport during the twentieth century, which is derived from the observed sea level data recorded by coastal tidal gauges, and they provided direct observational evidence supporting that the Atlantic Ocean integrates the NAO atmospheric variability and responds by causing changes in the AMOC and associated ocean heat transport with a time lag of about one decade (Li et al. 2013; Sun et al. 2015b; Gulev and Latif 2015). Thus, the iNAO represents the accumulated effect of NAO atmospheric forcing on the ocean circulation and thus can be used as a proxy for the AMOC.

As shown in Fig. 9b, the iNAO varies strongly in phase with the AMO at decadal timescales. The correlation of the iNAO with the AMO at decadal timescales is highly positive and significant (r = 0.85). The strong coherence between the iNAO and AMO is also observed for the NAO_{dif} (r = 0.89), and moreover, the averaged iNAO between the two NAO indices significantly covaries with the AMO, with the correlation reaching 0.91 (Fig. S3 of the Supplementary Material). Therefore, our results suggest that the decadal variability of observed AMO can be largely explained by the iNAO, and the observed NAO–AMO relationship can be also explained; that is, the accumulated effect of NAO forcing on the Atlantic Ocean gives rise to a decadal-scale lag between the NAO and AMO. This is consistent with the finding in McCarthy et al. (2015), but we extend the previous finding by a detailed comparison of different NAO

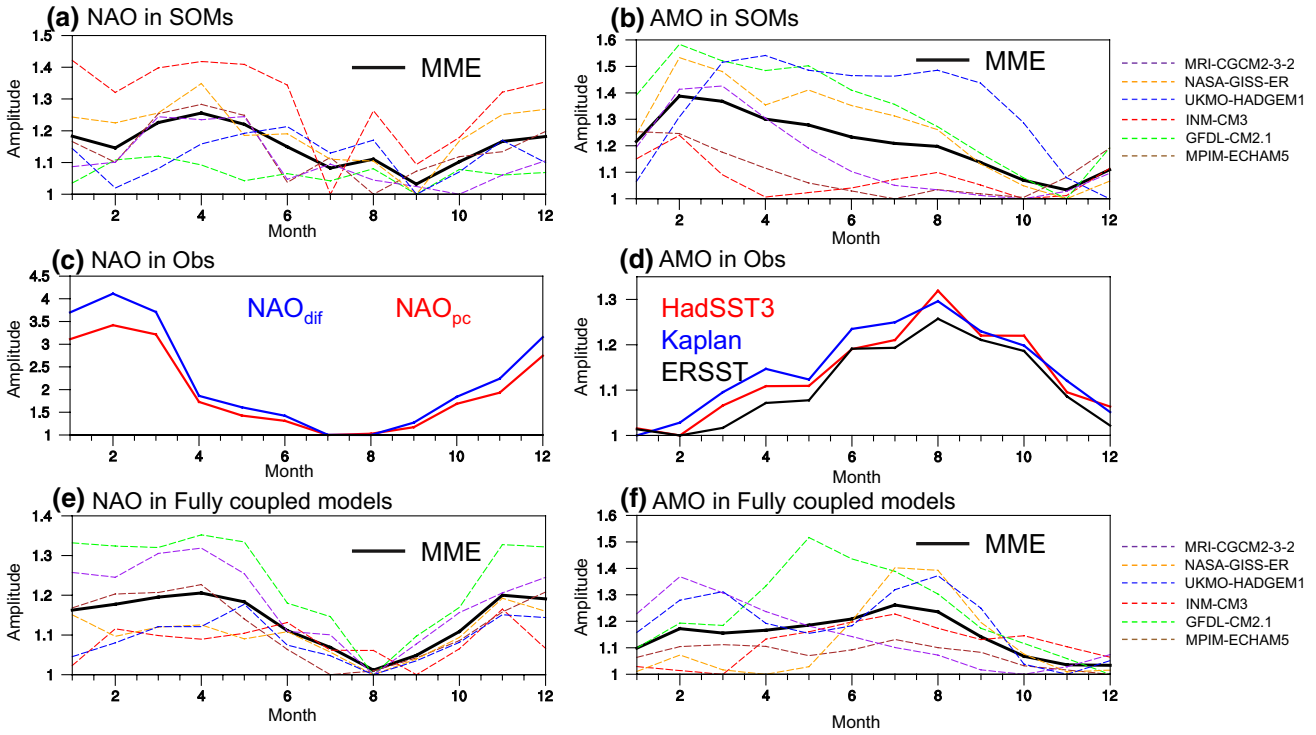

Fig. 7 **a** Annual cycle of the standard deviations of monthly NAO index as a function of calendar month based on the six slab ocean model simulations (dashed line in color) and the multi-model ensemble mean (black solid line). In each model, the standard deviations are divided by the minimum value across the calendar months. **b** As in **a**, but for the AMO$_s$ index. **c, d** As in **a** and **b**, respectively, but for the NAO and AMO indices in the observations. **e, f** As in **a** and **b**, respectively, but for the simulated NAO and AMO indices in the fully coupled models

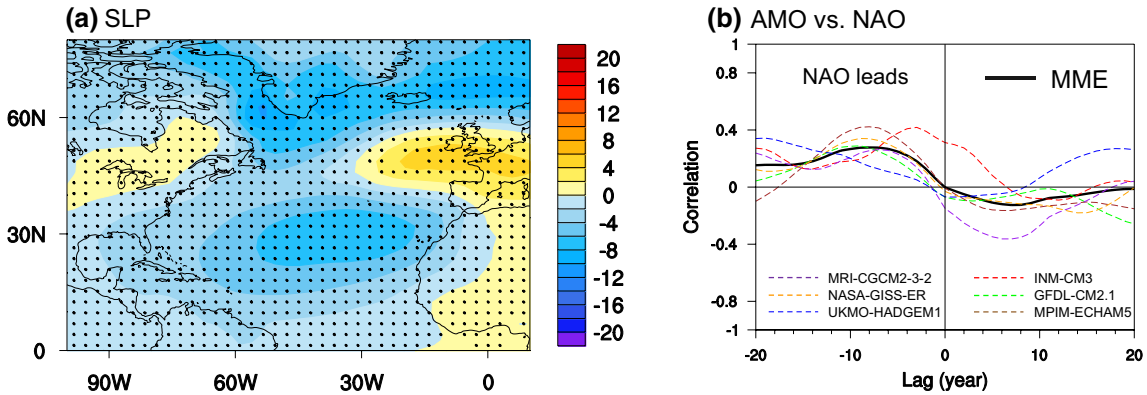

Fig. 8 **a, b** As in Fig. 4a, c, respectively, but for the results based on the six fully coupled model simulations

indices and by lengthening the analysis period prior to 1920. Since the iNAO is a good proxy for fluctuations in the North Atlantic ocean circulation, i.e., AMOC, we hypothesize that the AMOC may act as a common forcing signal that leads to a spatially consistent variation of SST over the entire North Atlantic basin.

To test this hypothesis, we conducted further analysis using the simulations from the fully coupled models. These simulations are the pre-industrial control integrations of the fully coupled version of the six SOMs and take into account ocean dynamics which are absent in the SOMs. The cross correlations of the Atlantic zonally average SST anomalies at various latitude represent the degree of spatial coherence of the SST variations, and the results based on simulations from the six fully coupled models are separately shown in Fig. 10. Consistent with

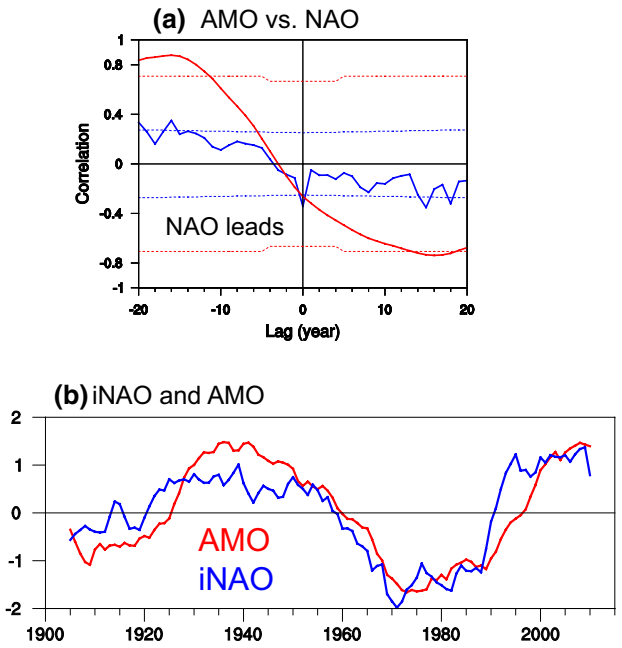

Fig. 9 The relationship between NAO and AMO in the observations. **a** Lead–lag correlations between the NAO and AMO indices for the period 1900–2015 based on decadally filtered (red) and unfiltered (blue) time series. Negative (positive) lags indicating the NAO leading (lagging) AMO. Red (blue) dashed lines denote the 95% confidence levels for filtered (unfiltered) time series using the effective numbers of degrees of freedom. **b** The decadally filtered AMO index and the time-integrated NAO (referred to as iNAO in the text) for the period 1900–2015. The two indices are scaled to unit variance and the long-term linear trends are removed

Fig. 2c, five out of the six models qualitatively reproduce the observed spatial synchronization of North Atlantic decadal SST variations, showing positive correlations of SST anomalies over the subpolar North Atlantic with those over the TNA and mid-latitude basin. The correlations between the TNA and mid-latitude SST anomalies are relative low, but remain positive in most models. This indicates a spatial synchronization of the decadal SST variations across the basin in the fully coupled models, and thus the SST anomalies share a common decadal-scale signal which can be represented by the spatial average, i.e. the AMO. An exception is the MRI-CGCM2-3-2 model, in which the mid-latitude SST anomalies are anticorrelated with those over the TNA and subpolar basin, similar to the results from SOMs. Nevertheless, it is clear that in the fully coupled models, the degree of spatial coherence of North Atlantic decadal SST variations is close to that in the observations and higher than that in the SOMs. The main difference between fully coupled models and SOMs is the inclusion of ocean dynamics, and thus the ocean dynamics may play an essential role in resulting in the spatial synchronization of SST variations across the basin.

The AMOC forces the spatially coherent SST anomalies associated with the AMO. Figure 11 shows the connection between the AMOC and AMO SST anomaly in the fully coupled models. For analysis involving AMOC, only four fully coupled models (indicated in Fig. 11) for which the data of AMOC streamfunction are available are included, and the strength of the simulated AMOC is defined as the maximum of the zonal mean meridional overturning streamfunction in the Atlantic at 30°N. We divide the four fully coupled models into two classes depending on the strength of the simulated AMOC–AMO relationship. We define Class-I models as those with a high correlation between AMOC and AMO, and three out of the four models fall into the Class-I models (indicated in Fig. 11a). All the three models simulate a strong AMOC–AMO relationship with a positive simultaneous correlation above 0.4. The positive correlation is not only simultaneous but is also stronger when the AMOC leads by 1–3 years, indicating that the AMOC forces the AMO SST anomalies at decadal timescales. This is generally consistent with the observational results based on the iNAO, a proxy for the AMOC. It is also noted that the three Class-I models fairly reproduce the spatial synchronization of decadal SST variations across the North Atlantic basin (Fig. 10). Meanwhile, only one model falls into the Class-II models which are defined as those with a low correlation between AMOC and AMO. The model is MRI-CGCM2-3-2, in which the simulated AMOC–AMO relationship is much weaker than the Class-I models (Fig. 11b) and the forcing of North Atlantic SST by the AMOC is negligible. The MRI-CGCM2-3-2 model also fails to reproduce the spatial coherence of decadal SST variations across the basin (Fig. 10). Therefore, a comparison between Class-I and Class-II models indicates that only a model that properly simulates the AMOC–AMO relationship can reproduces the observed spatial coherence of North Atlantic decadal SST anomalies. The forcing of SST anomalies by the AMOC-related ocean dynamics is crucial for the basin-wide uniform structure of the AMO. As shown in Fig. 11c, the AMOC is enhanced significantly during the warm AMO phase in the Class-I models, corresponding to a subsequent increase in the northward ocean heat transport which leads to SST warming over the entire basin. Thus, the above results provide direct modeling evidence that the AMOC acts as a common forcing signal that leads to a spatially coherent variation of North Atlantic SST.

The above analyses based on both observations and simulations identify the spatial coherence of AMO SST anomalies as a key feature that can be used to distinguish the AMO mechanism. Meanwhile, this unique feature of AMO also has important implications for understanding the climate impacts of AMO. Figure 12 shows the LSAT anomalies associated with the AMO over the continental

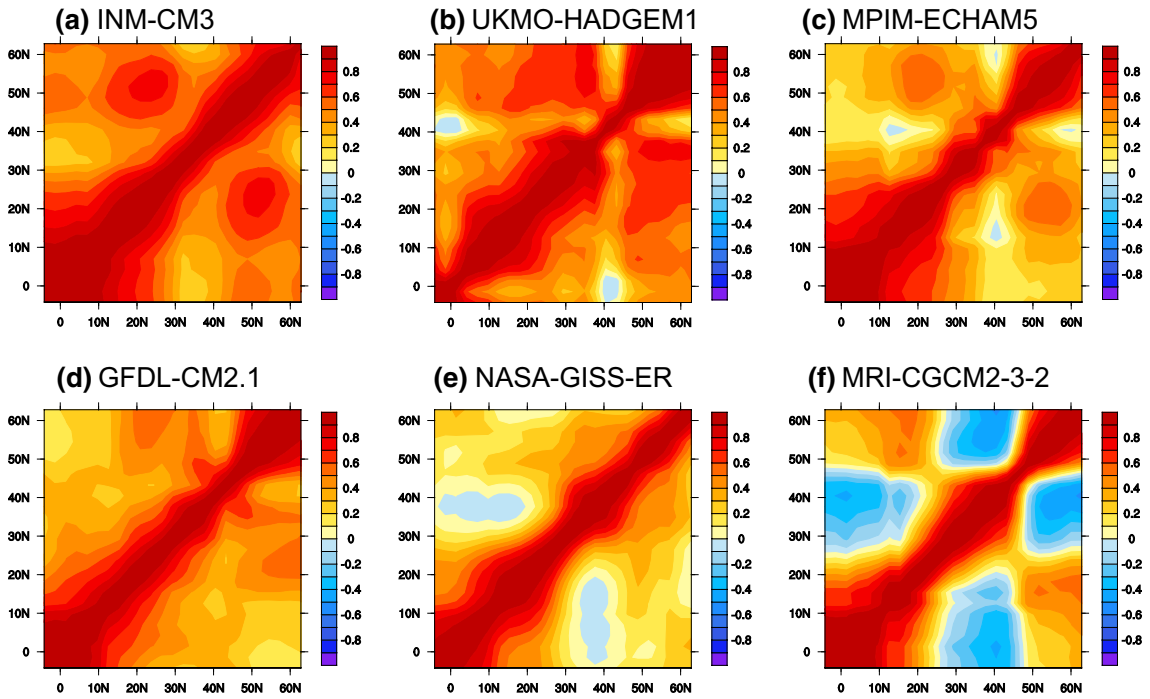

Fig. 10 Cross-correlation coefficients between decadally filtered zonal-average SST anomalies over the North Atlantic (80°W–0°) based on the six fully coupled model simulations

regions surrounding North Atlantic basin in the observations and SOM simulations. In both CRU and UDEL data sets, coherent LSAT warming is observed over the eastern North America, southern Greenland, western Europe and western Africa in association with the warm AMO phase. This coherent LSAT warming pattern across the regions surrounding the Atlantic Ocean is mainly thermodynamically driven by the basin-wide uniform SST anomalies of AMO (Sutton and Dong 2012; O'Reilly et al. 2016, 2017). In contrast, the simulated LSAT anomalies associated with the AMO in most of the SOMs exhibit a different pattern, with LSAT cooling over the southeastern North America and northwestern Europe and LSAT warming over other continental regions surrounding the basin (Fig. 12c). This anomalous LSAT pattern is somewhat similar to the negative phase of NAO (Hurrell 1995), and the LSAT cooling over the southeastern North America is consistent with the cool SST anomaly over the GSE region of the AMO_s tripole-like pattern. This suggests that the SOMs also fail to reproduce the observed influence of AMO on the LSAT. Most of the fully coupled models correctly reproduce the observed LSAT warming pattern, and this is probably due to a reasonable skill of the fully coupled models to simulate the observed spatial coherence of AMO (Fig. 12d). Thus, the spatial coherence of AMO SST anomalies is essential for understanding the consistent LSAT response across the regions surrounding the Atlantic Ocean.

4 Conclusion and discussion

The recently proposed atmosphere-forced thermodynamics mechanism (Clement et al. 2015, 2016; Cane et al. 2017) challenged the well-known ocean dynamics mechanism, and thus it is important to identify a key feature associated with the AMO that can be used to distinguish between the two mechanisms. In this study, the spatial structure of AMO is analyzed and compared between the observations and simulations from slab ocean models and fully coupled models. The observed SST pattern of AMO is characterized by a basin-wide monopole structure, and there is a significantly high degree of spatial coherence of decadal SST variations across the entire North Atlantic basin. The observed SST anomalies over North Atlantic share a common decadal-scale signal, corresponding to the basin-wide average (i. e., the AMO). In contrast, the simulated AMO in slab ocean models (referred to as AMO_s) exhibits a tripole-like structure, with the mid-latitude North Atlantic SST showing an inverse relationship with other parts of the basin, and the slab ocean models fail to reproduce the strong spatial coherence of decadal SST variations associated with the AMO.

The spatial coherence of AMO SST anomalies is identified as a key feature that can be used to distinguish the AMO mechanism. The tripole-like SST pattern of AMO_s in slab ocean models can be largely explained by the atmosphere-forced thermodynamics mechanism due to the surface turbulent heat flux changes associated with the NAO. A negative

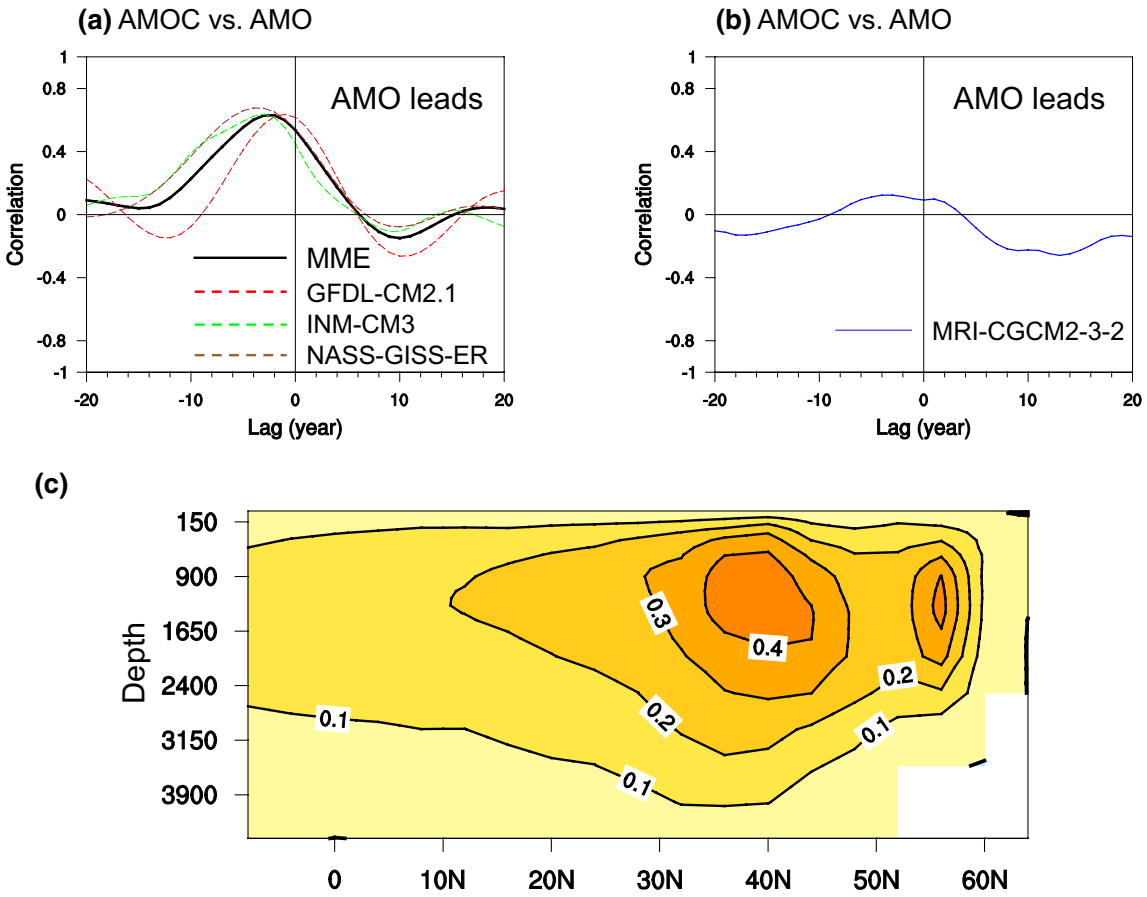

Fig. 11 **a** Lead–lag correlations between the AMOC and AMO indices at decadal timescales in three fully coupled models (dashed lines in color) and the multi-model ensemble mean (black solid line). Negative (positive) lags indicate the AMOC leading (lagging) the AMO. **b** Lead–lag correlation between the AMOC and AMO indices at decadal timescales in the MRI-CGCM2-3-2 model. **c** Multi-model ensemble mean regression of AMOC streamfunction anomalies (Sv) onto the normalized AMO index at decadal timescales based on the three fully coupled model simulations in **a**

(positive) NAO leads to anomalous heat flux out of (into) the ocean surface over the mid-latitude North Atlantic while downward (upward) surface heat flux anomalies over other parts of the basin. The thermodynamic forcing of AMO_s by the NAO gives rise to a simultaneous inverse NAO–AMO_s relationship at both interannual and decadal timescales and a seasonal phase locking of the AMO_s variability to the cold season. However, the NAO-forced thermodynamics mechanism cannot explain the observed NAO–AMO relationship and the seasonal phase locking of observed AMO variability to the warm season. At decadal timescales, there is a strong lagged relationship between observed NAO and AMO, with the NAO leading by up to two decades, and the simultaneous correlation of NAO with AMO is weak and insignificant. This lagged relationship can be well understood from the view point of AMOC-related ocean dynamics. A time-integrated NAO index, which reflects the variations in AMOC and northward ocean heat transport caused by the accumulated effect of NAO forcing, reasonably well captures the observed multidecadal fluctuations in the AMO. Further analysis using the fully coupled model simulations provides direct modeling evidence that the observed spatial coherence of decadal SST variations across North Atlantic basin can be reproduced only by including the AMOC-related ocean dynamics and the AMOC acts as a common forcing signal that results in a spatially coherent variation of North Atlantic SST.

This study highlights that the ocean dynamics mechanism plays a dominant role in shaping a basin-wide coherent SST pattern of the AMO and provides observational evidence that the AMO and relevant ocean dynamical process are closely related to the NAO at decadal timescales. There has been substantial modeling evidence that the simulated responses of AMOC and AMO lag the NAO forcing by years to decades (Eden and Jung 2001; Sun et al. 2015b; Delworth and Zeng 2016; Delworth et al. 2016, 2017). Recent studies based on current CMIP5 fully coupled models have suggested that there are a number of models in which the

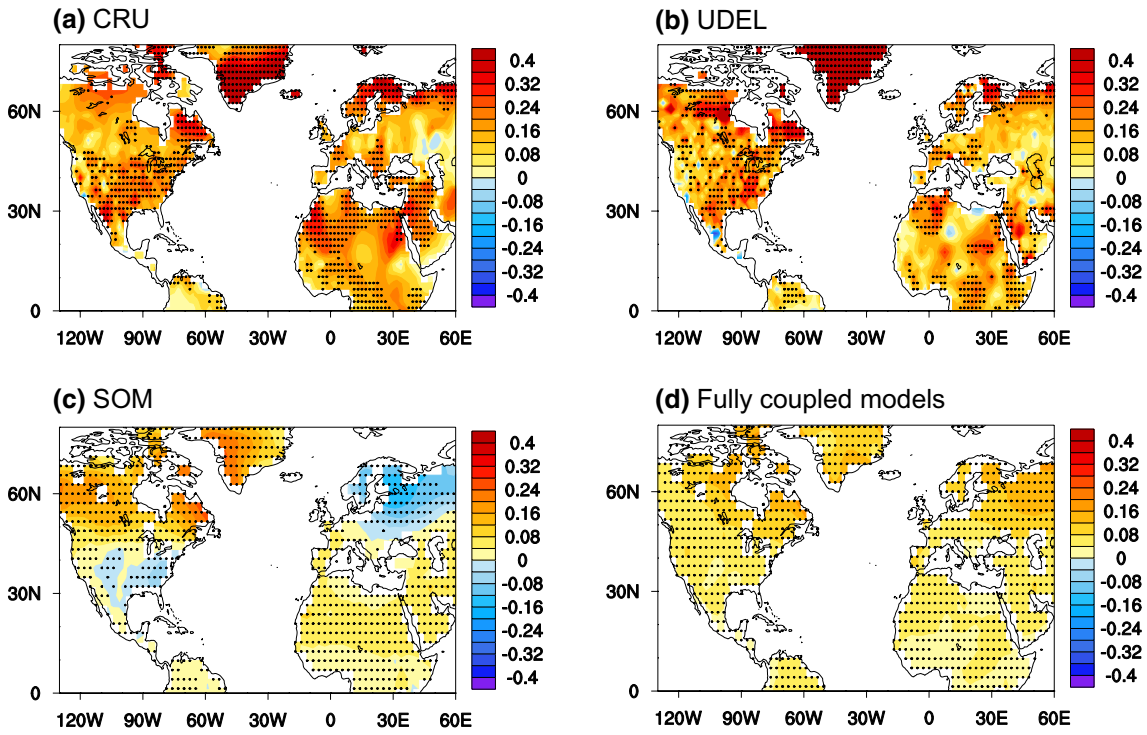

Fig. 12 **a** Regression map of land surface air temperature anomalies (K) onto the normalized AMO index at decadal timescales for the period 1901–2014 based on the CRU data set. **b** As in **a**, but based on the UDEL data set for the period 1901–2010. Dots in **a** and **b** stand for the regression coefficients significant at the 95% confidence level. **c** Multi-model ensemble mean regression of decadally filtered land surface air temperature anomalies onto the normalized AMO index based on the six slab ocean model simulations. **d** As in **c**, but based on the six fully coupled model simulations. Dots in **c** and **d** denote the area where at least four of the six models agree on the sign of the regressions

lagged correlation between decadal NAO and AMO is qualitatively similar to that observed (Peings et al. 2016; Wang et al. 2017). This indicates that there may be some improvement in the simulation of the NAO–AMO relationship from CMIP3 to CMIP5 models. Thus, in order to identify the key process influencing the NAO–AMO relation, a detailed and systematic comparison of the simulated relationship of NAO with AMO and AMOC between the CMIP3 and CMIP5 fully coupled models warrants further investigation. Meanwhile, this study focuses more on the NAO forcing effect on the AMO, but as shown in the NAO–AMO lead–lag correlations (a negative correlation found when the AMO leads NAO) and suggested by previous studies (Sun et al. 2015b; Peings et al. 2016), a two-way interaction may exist between the AMO and NAO at decadal time scales. In addition, this study investigates the SST signature of AMO only in the North Atlantic basin, while previous studies have suggested that the AMO signal can also be found in the southern ocean SST (Latif et al. 2006; Sun et al. 2013, 2015c). There is an interhemispheric seesaw pattern in decadal SST anomalies between North Atlantic and the southern ocean, and some modeling studies have suggested that this interhemispheric SST seesaw is linked to the AMOC-related ocean dynamics, i.e. meridional ocean heat transport (Latif et al. 2006; Keenlyside et al. 2008; Sun et al. 2015c). Therefore, the AMO signal in the southern oceans may provide another feature to further distinguish between the two mechanisms, and this issue deserves additional investigation in future studies.

Acknowledgements The authors wish to thank the anonymous reviewers for their constructive comments that significantly improved the quality of this paper. This work was jointly supported by the National Science Foundation of China (41775038, 41790474), National Key Research and Development Plan (2016YFA0601801) and the National Programme on Global Change and Air–Sea Interaction (GASI-IPOVAI-06 and GASI-IPOVAI-03).

References

Alexander MA, Halimeda Kilbourne K, Nye JA (2014) Climate variability during warm and cold phases of the Atlantic Multidecadal Oscillation (AMO) 1871–2008. J Mar Syst 133:14–26

Ba J, Keenlyside NS, Park W, Latif M, Hawkins E, Ding H (2013) A mechanism for Atlantic multidecadal variability in the Kiel Climate Model. Clim Dyn

Bellomo K, Murphy LN, Cane MA, Clement AC, Polvani LM (2017) Historical forcings as main drivers of the Atlantic multidecadal

variability in the CESM large ensemble. Clim Dyn. https://doi.org/10.1007/s00382-017-3834-3 **(in press)**
Booth BBB, Dunstone NJ, Halloran PR, Andrews T, Bellouin N (2012) Aerosols implicated as a prime driver of twentieth-century North Atlantic climate variability. Nature 484:228–232. https://doi.org/10.1038/nature10946
Cane MA, Clement AC, Murphy LN, Bellomo K (2017) Low-pass filtering, heat flux, and atlantic multidecadal variability. J Clim 30:7529–7553
Cayan DR (1992) Latent and sensible heat-flux anomalies over the Northern oceans—the connection to monthly atmospheric circulation. J Clim 5:354–369
Chen XY, Tung KK (2014) Varying planetary heat sink led to global-warming slowdown and acceleration. Science 345:897–903
Chen X, Wallace JM, Tung K-K (2017) Pairwise-rotated EOFs of global SST. J Clim 30:5473–5489
Clement A, Bellomo K, Murphy LN, Cane MA, Mauritsen T, Radel G, Stevens B (2015) The Atlantic multidecadal oscillation without a role for ocean circulation. Science 350:320-+
Clement A, Cane MA, Murphy LN, Bellomo K, Mauritsen T, Stevens B (2016) Response to comment on "the Atlantic Multidecadal Oscillation without a role for ocean circulation". Science 352(6293):1527. https://doi.org/10.1126/science.aaf2575
Delworth TL, Mann ME (2000) Observed and simulated multidecadal variability in the Northern Hemisphere. Clim Dyn 16:661–676
Delworth TL, Zeng FR (2016) The impact of the north atlantic oscillation on climate through its influence on the Atlantic meridional overturning circulation. J Clim 29:941–962
Delworth TL, Zhang R, Mann ME (2007) Decadal to centennial variability of the Atlantic from observations and models. In: Schmittner A, Chiang JCH, Hemming SR (eds) Past and future changes of the oceans meridional overturning circulation: mechanisms and impacts. Geophysical monograph series 173, American geophysical union, pp 131–148
Delworth TL, Zeng FR, Vecchi GA, Yang XS, Zhang LP, Zhang R (2016) The North Atlantic Oscillation as a driver of rapid climate change in the Northern Hemisphere. Nat Geosci 9:509
Delworth TL, Zeng F, Zhang L, Zhang R, Vecchi GA, Yang X (2017) The central role of ocean dynamics in connecting the north Atlantic oscillation to the extratropical component of the Atlantic multidecadal oscillation. J Clim 30:3789–3805
Deser C, Alexander MA, Timlin MS (2003) Understanding the persistence of sea surface temperature anomalies in midlatitudes. J Clim 16:57–72
Deser C, Alexander MA, Xie S-P, Phillips AS (2010) Sea surface temperature variability: patterns and mechanisms. Annu Rev Mar Sci 2:115–143
Dijkstra HA, Raa L, Schmeits M, Gerrits J (2006) On the physics of the Atlantic Multidecadal Oscillation. Ocean Dyn 56:36–50
Drews A, Greatbatch RJ (2016) Atlantic multidecadal variability in a model with an improved North Atlantic current. Geophys Res Lett 43:8199–8206
Eden C, Jung T (2001) North Atlantic interdecadal variability: oceanic response to the North Atlantic oscillation (1865–1997). J Clim 14:676–691
Enfield DB, Mestas-Nunez AM, Trimble PJ (2001) The Atlantic multidecadal oscillation and its relation to rainfall and river flows in the continental US. Geophys Res Lett 28:2077–2080
García-Serrano J, Cassou C, Douville H, Giannini A, Doblas-Reyes FJ (2017) Revisiting the ENSO teleconnection to the tropical North Atlantic. J Clim 30:6945–6957
Gray ST (2004) A tree-ring based reconstruction of the Atlantic multidecadal oscillation since 1567 A.D. Geophys Res Lett 31
Gulev SK, Latif M (2015) Ocean Science: the origins of a climate oscillation. Nature 521:428–430
Gulev SK, Latif M, Keenlyside N, Park W, Koltermann KP (2013) North Atlantic Ocean control on surface heat flux on multidecadal timescales. Nature 499:464–467
Harris I, Jones PD, Osborn TJ, Lister DH (2014) Updated high-resolution grids of monthly climatic observations—the CRU TS3.10 Dataset. Int J Climatol 34:623–642
Hurrell JW (1995) Decadal trends in the North-Atlantic oscillation—regional temperatures and precipitation. Science 269:676–679
Kaplan A, Cane MA, Kushnir Y, Clement AC, Blumenthal MB, Rajagopalan B (1998) Analyses of global sea surface temperature 1856–1991. J Geophys Res Oceans 103:18567–18589
Keenlyside NS, Latif M, Jungclaus J, Kornblueh L, Roeckner E (2008) Advancing decadal-scale climate prediction in the North Atlantic sector. Nature 453:84–88
Kennedy JJ, Rayner NA, Smith RO, Parker DE, Saunby M (2011) Reassessing biases and other uncertainties in sea surface temperature observations measured in situ since 1850: 1. Measurement and sampling uncertainties. J Geophys Res Atmos 116:D14103. https://doi.org/10.1029/2010JD015218
Knight JR, Allan RJ, Folland CK, Vellinga M, Mann ME (2005) A signature of persistent natural thermohaline circulation cycles in observed climate. Geophys Res Lett 32
Knight JR, Folland CK, Scaife AA (2006) Climate impacts of the Atlantic Multidecadal Oscillation. Geophys Res Lett 33
Kucharski F, Parvin A, Rodriguez-Fonseca B, Farneti R, Martin-Rey M, Polo I, Mohino E, Losada T, Mechoso CR (2016) The teleconnection of the tropical Atlantic to Indo-Pacific sea surface temperatures on inter-annual to centennial time scales: a review of recent findings. Atmosphere 7:29
Latif M, Collins M, Pohlmann H, Keenlyside N (2006) A review of predictability studies of Atlantic sector climate on decadal time scales. J Clim 19:5971–5987
Li S, Bates GT (2007) Influence of the Atlantic Multidecadal Oscillation on the winter climate of East China. Adv Atmos Sci 24:126–135
Li JP, Wang JXL (2003) A new North Atlantic Oscillation index and its variability. Adv Atmos Sci 20:661–676
Li JP, Sun C, Jin FF (2013) NAO implicated as a predictor of Northern Hemisphere mean temperature multidecadal variability. Geophys Res Lett 40:5497–5502
Li X, Xie S-P, Gille ST, Yoo C (2015) Atlantic-induced pan-tropical climate change over the past three decades. Nat Clim Change 6:275–279
Lu RY, Dong BW, Ding H (2006) Impact of the Atlantic multidecadal oscillation on the Asian summer monsoon. Geophys Res Lett 33
Marshall J, Kushner Y, Battisti D, Chang P, Czaja A, Dickson R, Hurrell J, McCartney M, Saravanan R, Visbeck M (2001) North Atlantic climate variability: phenomena, impacts and mechanisms. Int J Climatol 21:1863–1898
McCabe GJ, Palecki MA (2006) Multidecadal climate variability of global lands and oceans. Int J Climatol 26:849–865
McCarthy GD, Haigh ID, Hirschi JJ, Grist JP, Smeed DA (2015) Ocean impact on decadal Atlantic climate variability revealed by sea-level observations. Nature 521:508–510
Mecking JV, Keenlyside NS, Greatbatch RJ (2013) Stochastically-forced multidecadal variability in the North Atlantic: a model study. Clim Dyn 43:271–288
Mecking JV, Keenlyside NS, Greatbatch RJ (2015) Multiple timescales of stochastically forced North Atlantic Ocean variability: a model study. Ocean Dyn 65:1367–1381
Murphy LN, Bellomo K, Cane M, Clement A (2017) The role of historical forcings in simulating the observed Atlantic multidecadal oscillation. Geophys Res Lett 44:2472–2480
O'Reilly CH, Huber M, Woollings T, Zanna L (2016) The signature of low-frequency oceanic forcing in the Atlantic Multidecadal Oscillation. Geophys Res Lett 43:2810–2818

O'Reilly CH, Woollings T, Zanna L (2017) The dynamical influence of the Atlantic Multidecadal Oscillation on continental climate. J Clim 30:7213–7230

Ottera OH, Bentsen M, Drange H, Suo LL (2010) External forcing as a metronome for Atlantic multidecadal variability. Nat Geosci 3(10):688–694

Parker D, Folland C, Scaife A, Knight J, Colman A, Baines P, Dong BW (2007) Decadal to multidecadal variability and the climate change background. J Geophys Res Atmos 112

Peings Y, Simpkins G, Magnusdottir G (2016) Multidecadal fluctuations of the North Atlantic Ocean and feedback on the winter climate in CMIP5 control simulations. J Geophys Res Atmos 121:2571–2592

Robson J, Sutton R, Lohmann K, Smith D, Palmer MD (2012) Causes of the rapid warming of the North Atlantic ocean in the mid-1990s. J Clim 25:4116–4134

Schlesinger ME, Ramankutty N (1994) An oscillation in the global climate system of period 65–70 years. Nature 367:723–726

Smith TM, Reynolds RW, Peterson TC, Lawrimore J (2008) Improvements to NOAA's historical merged land–ocean surface temperature analysis (1880–2006). J Clim 21:2283–2296

Stocker TF, Qin D, Plattner GK, Tignor M, Allen SK, Boschung J, Nauels A, Xia Y, Bex B, Midgley BM (2013) Climate change 2013: the physical science basis intergovernmental panel on climate change, working group I contribution to the IPCC fifth assessment report (AR5). Cambridge University Press, New York

Sun C, Li JP, Jin FF, Ding RQ (2013) Sea surface temperature interhemispheric dipole and its relation to tropical precipitation. Environ Res Lett 8:044006

Sun C, Li J, Zhao S (2015a) Remote influence of Atlantic multidecadal variability on Siberian warm season precipitation. Sci Rep 5:16853

Sun C, Li J, Jin F-F (2015b) A delayed oscillator model for the quasi-periodic multidecadal variability of the NAO. Clim Dyn 1–17

Sun C, Li JP, Feng J, Xie F (2015c) A decadal-scale teleconnection between the North Atlantic oscillation and subtropical eastern Australian rainfall. J Clim 28:1074–1092. https://doi.org/10.1175/JCLI-D-14-00372.1

Sun C, Li JP, Ding RQ, Jin Z (2017a) Cold season Africa–Asia multidecadal teleconnection pattern and its relation to the Atlantic multidecadal variability. Clim Dyn 48:3903–3918

Sun C, Kucharski F, Li JP, Jin FF, Kang IS, Ding RQ (2017b) Western tropical Pacific multidecadal variability forced by the Atlantic multidecadal oscillation. Nat Commun 8:15998

Sutton RT, Dong BW (2012) Atlantic Ocean influence on a shift in European climate in the 1990s. Nat Geosci 5:788–792

Sutton RT, Hodson DLR (2005) Atlantic Ocean forcing of North American and European summer climate. Science 309:115–118

Ting MF, Kushnir Y, Seager R, Li CH (2009) Forced and internal Twentieth-Century SST Trends in the North Atlantic. J Clim 22:1469–1481

Trenberth KE, Shea DJ (2006) Atlantic hurricanes and natural variability in 2005. Geophys Res Lett 33

Trenberth KE, Paolino DA (1980) The northern hemisphere sea-level pressure data set: trends, errors and discontinuities. Mon Weather Rev 108:855–872

Vecchi GA, Delworth TL (2017) Integrate the whole system. Nature 548:284

Wang C, Dong S, Munoz E (2009) Seawater density variations in the North Atlantic and the Atlantic meridional overturning circulation. Clim Dyn 34:953–968

Wang XF, Li JP, Sun C, Liu T (2017) NAO and its relationship with the Northern Hemisphere mean surface temperature in CMIP5 simulations. J Geophys Res Atmos 122:4202–4227

Willmott CJ, Matsuura K (2001) Terrestrial air temperature and precipitation: monthly and annual time series (1950–1999) Version 1.02

Zhang R (2008) Coherent surface-subsurface fingerprint of the Atlantic meridional overturning circulation. Geophys Res Lett 35:L20705. https://doi.org/10.1029/2008GL035463

Zhang R (2017) On the persistence and coherence of subpolar sea surface temperature and salinity anomalies associated with the Atlantic multidecadal variability. Geophys Res Lett 44:7865–7875

Zhang R, Delworth TL (2007) Impact of the Atlantic multidecadal oscillation on North Pacific climate variability. Geophys Res Lett 34(23):L23708. https://doi.org/10.1029/2007GL031601

Zhang L, Wang C (2013) Multidecadal North Atlantic sea surface temperature and Atlantic meridional overturning circulation variability in CMIP5 historical simulations. J Geophys Res Oceans 118:5772–5791

Zhang R, Delworth TL, Sutton R, Hodson DLR, Dixon KW, Held IM, Kushnir Y, Marshall J, Ming Y, Msadek R, Robson J, Rosati AJ, Ting M, Vecchi GA (2013) Have aerosols caused the observed Atlantic multidecadal variability? J Atmos Sci 70:1135–1144

Zhang R, Sutton R, Danabasoglu G, Delworth TL, Kim WM, Robson J, Yeager SG (2016) Comment on "The Atlantic Multidecadal Oscillation without a role for ocean circulation". Science 352